Gene expression profiling of the astrocyte transcriptome in multiple sclerosis normal appearing white matter reveals a neuroprotective role

WALLER, Rachel, WOODROOFE, Nicola <http://orcid.org/0000-0002-8818-331X>, WHARTON, Stephen B., INCE, Paul G., FRANCESE, Simona <http://orcid.org/0000-0002-1381-1262>, HEATH, Paul R., CUDZICH-MADRY, A, THOMAS, Ruth, ROUNDING, Natalie, SHARRACK, Basil and SIMPSON, Julie E.

Gene expression profiling of the astrocyte transcriptome in multiple sclerosis normal appearing white matter reveals a neuroprotective role

Authors:
Rachel Waller [a], M. Nicola Woodroofe [b], Stephen B. Wharton [a], Paul G. Ince [a], Simona Francese [b], Paul R. Heath [a], Alex Cudzich-Madry[b], Ruth H. Thomas[b], Natalie Rounding [a], Basil Sharrack [a,c] *, Julie E. Simpson [a]*

Affiliations:
[a] Sheffield Institute for Translational Neuroscience, University of Sheffield, UK
[b] Biomolecular Sciences Research Centre, Sheffield Hallam University, UK
[c] Department of Neurology, Royal Hallamshire Hospital, Sheffield, UK

* Joint senior authors

Corresponding author:
Dr Julie Simpson
Sheffield Institute for Translational Neuroscience
385A Glossop Road
Sheffield, UK
S10 2HQ
Tel: +44 (0) 114 222 2242
Fax: +44 (0) 114 222 2290
Email: julie.simpson@sheffield.ac.uk

Abstract

Multiple sclerosis (MS) is a chronic, inflammatory, demyelinating disease of the central nervous system (CNS). White matter lesions in MS are surrounded by areas of non-demyelinated normal appearing white matter (NAWM) with complex pathology, including blood brain barrier dysfunction, axonal damage and glial activation. Astrocytes, the most abundant cell type within the CNS, may respond and/or contribute to lesion pathogenesis. We aimed to characterise the transcriptomic profile of astrocytes in NAWM to determine whether specific glial changes exist in the NAWM which contribute to lesion development or prevent disease progression.

Astrocytes were isolated from control and NAWM by laser capture microdissection (LCM), using glial fibrillary acidic protein (GFAP) as a marker, and the astrocyte transcriptome determined using microarray analysis. 452 genes were significantly differentially expressed (208 up-regulated and 244 down-regulated, FC≥1.5 and p-value≤0.05). Within the NAWM, astrocytes were associated with significant upregulation of genes involved in the control of iron homeostasis (including metallothionein-1 and -2, ferritin light chain and transferrin), oxidative stress responses, the immune response and neurotrophic support. These findings suggest a neuroprotective role of astrocytes in the NAWM in MS.

Keywords:

multiple sclerosis, normal appearing white matter, astrocyte, neuroprotection, microarray

Highlights:

- GFAP is the optimal marker to label astrocytes for laser capture microdissection
- Astrocytes in the NAWM express transcripts associated with iron homeostasis
- Astrocytes increase expression of oxidative stress & immune response-related genes

1. Introduction

Multiple sclerosis (MS) is a complex disease neuropathologically characterised by demyelinated lesions distributed throughout the brain and spinal cord, inflammation, axonal/neuronal damage, gliosis, oxidative stress, excitotoxicity and blood brain barrier (BBB) dysfunction (Stables et al., 2010). Subtle pathological changes exist in the normal appearing white matter (NAWM) that are not detected by standard magnetic resonance imaging (MRI) and are only identifiable upon immunohistochemical evaluation, including mild inflammation, microglial activation, astrogliosis, axonal swelling, cellular infiltration and reduced myelin density (Moll et al., 2011, Allen et al., 2001, Allen and McKeown, 1979, Kutzelnigg et al., 2005, Lund et al., 2013). The cause of these changes in the white matter in MS are unknown but may be a result of underlying molecular pathology, or they may represent lesions that are beyond the sensitivity of current imaging techniques (Mistry et al., 2011). In order to better understand the pathogenesis of the disease and the mechanisms underlying lesion development, the processes that occur within the surrounding NAWM need to be identified.

Astrocytes play a key role in maintaining the extracellular environment and supporting neurons (Sobel & Moore 2008). While it has been suggested that astrocytes play a neuroprotective role in MS by inhibiting demyelination (Miljkovic et al., 2011), releasing anti-inflammatory cytokines (Bsibsi et al., 2006) and secreting proteins involved in myelin repair and neurotrophins to support regeneration of neurons (Marz et al., 1999, Moore et al., 2011a, Moore et al., 2011b, Mason et al., 2001, Miljkovic et al., 2011), it has also been proposed that astrocytes are detrimental in disease pathogenesis by releasing pro-inflammatory cytokines, contributing to BBB dysfunction (Argaw et al., 2006, Argaw et al., 2012) and preventing oligodendrocyte precursor cell (OPC) maturation into remyelinating oligodendrocytes (Messersmith et al., 2000, Sarchielli et al., 2008).

The advancement of transcriptomic technology enables studies to be carried out to identify the genetic profile associated with the pathogenesis of disease. To date, gene expression profiling in MS has focussed on the differences between demyelinated lesions and neurological control WM, as reviewed (Dutta and Trapp, 2012, Dutta, 2013). MS is a heterogeneous and progressive disease where the architecture of the brain tissue is constantly changing depending on the stage of the disease (Bradl and Lassmann, 2012). Consequently, investigating NAWM as opposed to established lesions may identify factors that initiate or prevent disease progression compared to the genetic profile of an already established demyelinated lesion. Yet despite this, to date only four microarray studies have investigated the gene expression profile of NAWM in MS (Graumann et al., 2003, Lindberg et al., 2004, Zeis et al., 2008, Mycko et al., 2012) with transcriptomic changes identified in whole tissue, constituting a heterogeneous cell population.

Laser capture microdissection (LCM) allows the isolation of particular regions or cells of interest from post-mortem material and can be used in conjunction with microarray analysis to identify differentially expressed genes in an enriched cell population. To date, only two studies have combined LCM with microarray analysis in MS research, including analysis of the gene expression profile of blood vessels (Cunnea et al., 2010) and LCM-ed areas of MS lesions and NAWM (Mycko et al., 2012).

Transcriptomic profiling of astrocytes in the NAWM in MS may identify disease relevant gene expression changes and elucidate pathological processes that can be manipulated through therapeutic intervention at an earlier stage in the disease, preventing lesion development and ultimately disease progression. Therefore, the current study used immuno-guided LCM to isolate astrocytes from NAWM and control WM, followed by gene expression profiling. Our findings identify the major astrocyte-associated gene differences between NAWM and control WM and highlights novel candidate genes. This contributes to our understanding of the potential role of astrocytes in restricting MS lesion development.

2. Materials and Methods

2.1 Human central nervous system (CNS) tissue

CNS tissue was obtained from the UK Multiple Sclerosis Tissue Bank Wales Research Ethics Committee (Ref. No. 08/MRE09/31). Snap frozen NAWM and control WM samples used in the microarray study were selected based on their neuropathological assessment and, where possible, the cases were matched for age and gender (Table 1). The ribosomal integrity number (RIN) of each frozen tissue block was assessed prior to LCM using a previously reported method (Bahn et al., 2001, Waller et al., 2012). Only samples with a pre-LCM RIN >3.0 and brain pH >6.5 were taken forward for immuno-LCM. The quantity of RNA from each sample was analysed using a NanoDrop 1000 spectrophotometer (Thermoscientific, UK) and the quality of RNA assessed on a 2100 bioanalyzer (Agilent, Palo Alto, CA, USA).

2.2 Immunohistochemistry

To determine the most suitable astrocyte marker that clearly labelled individual astrocytes for use in immuno-guided LCM and to visualise the proteins encoded by key candidate genes, immunohistochemistry (IHC) was performed using a standard avidin-biotin complex (ABC) method with diaminobenzidine (DAB) as substrate (Vector Laboratories, UK) (Table 2 lists the antibodies used). Negative controls including isotype-specific antibody controls and the omission of the primary antibody confirmed the specificity of staining. Dual labelling with the astrocyte marker GFAP was performed as previously described (Fluteau et

al., 2015) to investigate astrocyte association with FTL. Images were acquired using a BX61 Olympus microscope and CellR image software.

2.3 Immuno-laser capture microdissection (LCM) of astrocytes and RNA extraction

Astrocytes were isolated using a rapid immuno-LCM method, as previously described in detail (Waller et al., 2012). Approximately 1,000 glial fibrillary acidic protein ($GFAP^+$) astrocytes were isolated from each case using the PixCell II laser capture microdissection system (Arcturus Engineering, Mountain View, CA, USA). Total RNA was extracted using the PicoPure RNA isolation kit, according to the manufacturer's instructions (Arcturus BioScience, UK). The quantity and quality of the extracted RNA was determined using a Nanodrop 1000 spectrophotometer (Thermoscientific, UK) and a 2100 Bioanalyzer, respectively (Agilent, USA). Only those samples identified as having a RIN >2.0 post-LCM were taken forward for microarray analysis.

2.4 RNA amplification and microarray hybridization

The target labelled mRNA was prepared following the GeneChip 3' IVT Express amplification protocol (Affymetrix, UK). In brief, total RNA was reverse transcribed to synthesise the first-strand cDNA by annealing RNA with a T7 oligo(dT) primer. The single stranded cDNA was converted into double-stranded cDNA by a reaction with a DNA polymerase and RNase H. An overnight *in vitro* transcription (IVT), incorporating an IVT labelling master mix, allowed the synthesis of multiple copies of biotin-labelled antisense RNA from the double stranded cDNA template. Following clean-up and purification the quality of the labelled RNA was checked on the Agilent 2100 Bioanalyzer.

Approximately 6.5µg amplified labelled RNA was fragmented and hybridised to Affymetrix Human Genome U133 Plus 2.0 Array chips for 16 hours at 45°C in a rotating oven at 60rpm. Using the Fluidics Station 400, and Gene Chip Operating System, the hybridisation cocktail was removed and a series of washing steps followed to remove any unbound RNA, before each microarray was stained. Each microarray chip was scanned using the GeneChip 3000 scanner to determine the fluorescence intensity of hybridised transcripts.

2.5 Microarray analysis

The Affymetrix Gene Expression Console was used for quality and control analysis of the data, the image or .CEL files were imported to GeneSpring version 7.0 (Agilent, USA) and normalised to the median of all genes, prior to statistical analysis, to identify differentially expressed genes. Transcripts were defined as being significantly, differentially expressed if they showed a minimum fold change (FC) of >1.5 and a p-value of <0.05 (unpaired t-test).

Significantly, differentially expressed genes were classified according to their biological function using the Database for Annotation Visualisation and Integrated Discovery (DAVID) (Huang da et al., 2009a, Huang da et al., 2009b) and Kyto Encyclopedia of Genes and Genomes (KEGG) pathway analysis was carried out to identify specific pathways.

2.6 Validation of microarray data: quantitative real-time polymerase chain reaction (qPCR)

RNA was extracted from LCM-ed astrocytes from 9 additional frozen cases (4 control WM and 5 NAWM), which had not been used for the microarray studies. qPCR was performed using IDT PrimeTime qPCR assays (Integrated DNA Technologies, UK) containing 50 ng cDNA, 500nM primers, 250nM probe, and Brilliant qPCR mix (Agilent, UK) in a total volume of 10μl, for details of primer sequences see Table 3. Following denaturation at 95^{o}C for 3 min the products were amplified (40 cycles at 95^{o}C for 10s and 60^{o}C for 30s) using a CFX384 Touch^{TM} RT PCR detection system (Bio-Rad, UK). β-actin was amplified on each plate to normalise expression levels of target genes between different samples using the ΔΔCt calculation (ABI) and to assess assay reproducibility (Livak and Schmittgen, 2001).

3. Results

3.1 GFAP is currently the best marker of astrocytes for immuno-LCM

To determine the optimal marker of astrocytes to use for isolation using immuno-LCM, a panel of currently described astrocyte markers was employed. GFAP immunoreactivity was associated with the cell body and extending processes, and labelled astrocytes with a distinct stellate morphology (Figure 1a). S100B immunoreactivity was predominantly associated with astrocyte cell bodies, and was also associated with small, spherical cells morphologically resembling oligodendrocytes (Figure 1b). In comparison to antibodies against GFAP and S100B, which predominantly stained astrocyte cell bodies and immediate cell processes, both excitatory amino acid transporter-1 (EAAT1) (Figure 1c) and EAAT2 (Figure 1d) antibodies labelled the extending delicate processes of astrocytes, the pattern of which varied greatly across the sample cohort. In contrast, glutamine synthetase (GS) immunoreactivity was not as extensive as GFAP and was associated with the astrocyte cell body and immediate stumpy processes (Figure 1e). GS staining was not restricted to stellate astrocytes but also labelled the cytoplasm of small, spherical cells morphologically resembling oligodendrocytes. Aldehyde dehydrogenase 1 family member L1 (ALDH1L1) preferentially labelled cortical astrocytes, with little staining of WM. Within the cortex, ALDH1L1 immunoreactivity was restricted to the cell body and did not extend to the astrocyte processes, and was also associated with small spherical cells morphologically

resembling oligodendrocytes (Figure 1f). Based on astrocyte specificity, clear labelling of individual cells and ability to identify the maximum number of astrocytes, GFAP was selected as the best astrocyte marker for the further studies.

3.2 Confirmation of astrocyte enrichment

In order to confirm that the extracted RNA from each sample represented an enriched astrocyte population, specific transcript expressions were investigated. High levels of GFAP transcripts were found (astrocyte: probe set id 203540_at, mean signal intensity 5995.0; range, 1263.7-20549.3), but low levels of CD34 (endothelial cell: probe set id 209543_s_at, mean signal intensity 50.6; range, 14.7-98.4), CD68 (microglia: probe set id 203507_at, mean signal intensity 23.7; range, 4.1-64.1), and OLIG-2 oligodendrocyte: probe set id 213825_at, mean signal intensity 290.3; range, 133.5-520.7) confirming the extracted RNA from $GFAP^+$ LCM-ed cells represented an enriched astrocyte population. Moderately high levels of a neuronal transcripts were detected (NFL: probe set id 221805_at, mean signal intensity 3328.6; range, 368.9-5264.2), which may reflect the close proximity of astrocytes to axons.

3.3 NAWM associated changes in the astrocyte transcriptome

The transcription profiles of laser-captured astrocytes from NAWM and control WM were generated using Human Genome U133 Plus 2.0 Arrays, which comprise $1.3x10^6$ unique oligonucleotide sequences, including >47,000 transcripts and variants of 33,000 genes. Between 7.5% and 38.2% of the probe set sequences were present across all samples (mean [range]): NAWM (32.1% [22.5-36.4%]); control WM (26.6% [7.5-38.2%]).

Gene expression analyses are sensitive to the presence of sample outliers, therefore rigorous quality control procedures were used to ensure the highest possible level of quality for both datasets. Sample outliers were identified by visual inspection after clustering the samples using hierarchical clustering and 3 cases (MS5, C3 and C5) were removed from subsequent analysis (Figure 2). The robust multi-array average (RMA) was re-analysed after these cases were removed and principle component analysis was performed on the significant, differentially expressed genes of 4 NAWM and 3 control WM cases (the expression dataset is freely available at Gene Expression Omnibus, accession number GSE83670). Transcript clusters showed no association with age, gender, post-mortem delay or pH.

3,375 genes (1,778 up-regulated, 1,596 down-regulated) had altered expression in NAWM astrocytes compared to control astrocytes. Transcripts were deemed significantly, differentially expressed if they had a FC≥1.5 and a p-value≤0.05 (208 up-regulated and 244 down-regulated, (Supplementary Table 1). Functional grouping analysis identified that the

dysregulated genes were associated with the immune response, homeostasis, response to metal ion binding, response to hypoxia, cell signalling, cytoskeleton, RNA processing/protein metabolism, the cellular response to stress, the synapse, ubiquitin-mediated proteolysis, transport and transcription (Table 4).

3.3.1 Increased expression of transcripts associated with the regulation of iron homeostasis and the response to oxidative stress

Assessing the top 20 differentially upregulated genes (Table 5), identified 6 genes related to the regulation of iron homeostasis and the response to oxidative stress: metallothionein 1X [*MT1X*] probe set 208581_x_at, FC=2.23, p=0.042, metallothionein 1G [*MT1G*] probe set 204745_x_at, FC=2.26, p=0.031, metallothionein 2A [*MT2A*] probe set 212185_x_at, FC=2.52, p=0.032, metallothionein 1 pseudogene 2 [*MT1p2*] probe set 211456_x_at, FC=2.22, p=0.044, ferritin light chain [*FTL*] probe set 212788_x_at, FC=2.24, p=0.030, and transferrin [*TF*] probe set 214064_at, FC=2.21, p=0.048.

3.3.2 NAWM-associated increase in immune response-related transcripts

Functional grouping identified enrichment of genes associated with the immune response, with the majority of genes (15/19, Supplementary Table 1) upregulated in NAWM compared to control WM. These included CD74 (*CD74* probe set 209619_at, FC=2.73, p=0.008), complement component 1 (*C1QC* probe set 225353_s_at, FC=1.77, p=0.016), complement component 3 (*C3* probe set 217767_at, FC=1.94, p=0.035), interleukin-17C (*IL17C* probe set 224079_at, FC=1.54, p=0.039), interleukin-4 receptor (*IL4R* probe set 203233_at, FC=1.54, p=0.013), major histocompatibility complex class II (*HLA-DPA1* probe set 211990_at, FC=2.01, p=0.003) (*HLA-DPB1* probe set 201137_s_at, FC=1.85, p=0.006), prostaglandin-endoperoxide synthase 2 (*PTGS2* probe set 204748_at FC=-1.56, p=0.021 and transforming growth factor beta 3 (*TGF-B3* probe set209747_at, FC=1.55, p=0.024).

3.3.3 NAWM-associated dysregulation of signalling transcripts

Analysis of the astrocyte transcriptome in NAWM in MS also identified dysregulation of genes associated with multiple signalling pathways, including mitogen-activated protein kinase (MAPK) signalling [mitogen-activated protein kinase kinase kinase kinase 4 (*MAP4K4* probe set 218181_s_at, FC=1.54, p=0.016); mitogen-activated protein kinase-activated protein kinase 2 (*MAPKAPK2* probe set 201460_at, FC=1.70, p=0.039)], insulin signalling [insulin-like growth factor binding protein-5 (*IGFBP5* probe set 211959_at, FC=2.24, p=0.024; probe set 203424_s_at, FC=1.71, p=0.01)], calcium signalling [calcium channel, voltage dependent N-type, alpha 1B subunit (*CACNA1B* probe set 235781_at, FC=-1.68, p=0.039); calmodulin (*CALM1* probe set 211985_s_at, FC=-1.91, p=0.04)] and ubiquitin

signalling pathways [small ubiquitin-related modifier 1 (*SUMO1* probe set 203871_at, FC=-1.63, p=0.001); ubiquitin specific peptidase 43 (*USP43* probe set 237439_at, FC=-1.71, p=0.012)].

3.4 Validation of key gene expression changes

Astrocyte expression of the protein encoded by the candidate genes identified in the microarray study was confirmed by IHC. A regular pattern of ferritin light chain immunoreactivity was detected in all NAWM and control WM cases with staining associated with cells morphologically resembling microglia and astrocytes. Dual labelling confirmed a proportion of these ferritin light chain immunopositive cells were $GFAP^+$ astrocytes (Figure 3a). Calmodulin immunoreactivity was associated with the astrocyte cell bodies and immediate processes (Figure 3b). Dense metallothionein immunoreactivity was a common feature across all MS NAWM and control cases investigated, and was associated with the cell body and extending processes of cells with a typical astrocyte stellate morphology (Figure 3c). The altered expression of candidate genes was validated by qPCR on LCM-isolated astrocytes from additional cases. The NAWM was associated with significantly higher expression of *FTL* (p=0.008), and non-significant decreased expression of *CALM1*. (Figure 3d).

4. Discussion

Astrocytes play a key role in regulating homeostasis within the CNS, providing neurotrophic support, contributing to immune surveillance and maintaining BBB integrity (Pekny et al., 2015), with increasing evidence indicating a potential role of these glial cells in the pathogenesis of MS lesions (Brosnan and Raine, 2013). The radiologically normal WM surrounding these lesions is pathologically abnormal (Allen et al., 2001), and it is likely that identifying gene expression changes in astrocytes in the NAWM in MS may identify whether astrocytes contribute to, or prevent lesion initiation and progression. Several papers have discussed the complexity of astrocytes in MS, with emphasis on their dual function: on the one hand astrocytes are neurotoxic, through a deleterious immune response, increasing BBB permeability and inhibiting remyelination; whilst on the other these glial cells are neuroprotective, supporting oligodendrocyte remyelination and axonal regeneration (Williams et al., 2007, Nair et al., 2008, Brosnan and Raine, 2013). To date five studies have performed RNA profiling of the NAWM in MS compared to control WM, one recent study characterising the microRNA profile (Guerau-de-Arellano et al., 2015) and four studies have reported mRNA expression changes (Graumann et al., 2003, Lindberg et al., 2004, Zeis et al., 2008, Mycko et al., 2012). All of these studies were carried out using RNA from whole tissue extracts, which thus comprised a heterogeneous cell population within the

NAWM. To our knowledge, the current study is the first to perform microarray analysis on laser captured astrocytes from the NAWM, identifying increased expression of genes associated with the regulation of iron homeostasis, the response to oxidative stress, the immune response and neurotrophic support, suggesting a neuroprotective role of these cells in the NAWM in MS.

We have previously demonstrated that immuno-LCM of autopsy tissue enables the isolation and enrichment of specific cell populations for further downstream analysis (Waller et al., 2012). An increasing number of studies in a range of neurological diseases have used this approach to identify disease-relevant, cell-specific gene expression changes (Boone et al., 2013, Chu et al., 2009, Kumar et al., 2013, Pietersen et al., 2009, Simpson et al., 2011, Baker et al., 2015, Simpson et al., 2015). To date, only two studies have employed LCM in the investigation of human MS cases: one identifying gene expression changes in total extracts from NAWM, peri-lesional and lesional regions compared to control WM (Mycko et al., 2012) and the other identifying transcriptomic changes in the vascular compartment in MS (Cunnea et al., 2010); with neither study specifically assessing changes in the astrocyte transcriptome.

Iron is vital in the synthesis of myelin and neurotransmitters, and plays an important role in oxygen transport, DNA synthesis and repair, and mitochondrial energy production (Crichton et al., 2011, Todorich et al., 2009, Levenson and Tassabehji, 2004). Within the brain the majority of iron is present in the inactive ferric form (Fe^{3+}), with the remainder present in the active ferrous form (Fe^{2+}). Levels of iron within the CNS are strictly regulated as both deficient and excess concentrations impact cell viability (Li and Reichmann, 2016). Dysregulation of genes involved in the transport and storage of iron, including transferrin (*TF*) and ferritin (*FT*) respectively, leads to an increase in Fe^{3+} resulting in oxidative damage (Connor and Menzies, 1995). Increased iron deposition is associated with oligodendrocyte cytotoxicity and myelin loss in MS, with elevated levels detected at the peri-lesional margin (Bagnato et al., 2011, Hametner et al., 2013). Furthermore, excess iron can amplify microglial activation stimulating an increase in the secretion of pro-inflammatory cytokines, and can directly damage mitochondria resulting in increased oxidative stress (Williams et al., 2012, Haider et al., 2011).

Unlike oligodendrocytes and microglia, astrocytes are resilient to the cytotoxic effects of excess iron (Gaasch et al., 2007) which may, in part, be attributable to their increased expression of MT that scavenge transition metal ions and free radicals. Increased expression of MT by astrocytes forms part of the inflammatory and defence response, and has been reported in MS (Penkowa et al., 2003) and its animal model, experimental autoimmune encephalomyelitis (EAE) (Penkowa and Hidalgo, 2000, Espejo et al., 2005). MT treatment has also been shown to prevent demyelination and axonal damage, and

decrease expression of pro-inflammatory cytokines in EAE (Penkowa and Hidalgo, 2001, Penkowa and Hidalgo, 2003), providing direct evidence that increasing astrocytic expression of MT is a valid potential therapeutic target. The significant increased expression of iron regulatory genes identified in the current study, including MT1, MT2, FTL and TF, suggest a neuroprotective response whereby astrocytes adapt to protect the NAWM from widespread iron-induced oxidative damage.

The present study also revealed the significant upregulation of genes associated with the immune response, supporting previous gene expression studies performed on NAWM in MS (Lindberg et al., 2004). Interestingly there was no significant upregulation in expression of the pro-inflammatory cytokines interferon-γ or tumour necrosis factor-α, which are classically associated with the pathogenesis of MS (Kierdorf et al., 2010), but levels of *TGF-β3*, an astrocyte derived regulator of neuronal survival (Krieglstein et al., 2002), were significantly increased in the NAWM, suggesting a neuroprotective role for astrocytes in the NAWM. Furthermore, the current study identified significant downregulation of *PTGS2*, which encodes cyclooxygenase-2 (COX2), an enzyme which has been shown to stimulate the production of prostanoids that contribute to chronic inflammation (Minghetti, 2004), providing further support that astrocytes in the NAWM are neuroprotective.

Our analysis also revealed differential expression of genes associated with receptor mediated signalling pathways in NAWM, including MAPK and calcium signalling, confirming previous reports (Graumann et al., 2003, Zeis et al., 2008). The current study identified significant upregulation of *MAPKAPK2* and *MAPK4*, both of which are linked to ischaemic preconditioning and oxidative stress in MS (Graumann et al., 2003). Dysfunction of calcium signalling, calcium pumps and exchangers are linked to axonal injury and neuronal dysfunction in MS, where the abnormal influx, extrusion, buffering and sequestration results in a calcium imbalance which may initiate detrimental mechanisms (Kurnellas et al., 2007). Dysregulation of intracellular signalling pathways is also a feature of acute lesions (Whitney et al., 1999), active lesion margins (Mycko et al., 2012) and cortical pathology in MS (Dutta et al., 2007).

In this study we trialled a comprehensive panel of astrocyte markers and determined that immunolabelling for GFAP is currently the best approach to confidently visualise astrocytes for LCM isolation from post-mortem tissue. However, while GFAP is widely used as a reliable marker of astrocytes, it should be acknowledged that not all astrocytes are $GFAP^+$ (Sofroniew and Vinters, 2010), therefore our findings are biased towards the gene expression profile of the reactive astrocyte population. Furthermore, the technical limitations of LCM resulted in the isolation of an enriched, but not pure, population of $GFAP^+$ astrocytes. Transcriptomic analysis generates large datasets, therefore to limit the number of genes

submitted for analysis we examined genes that differed by a minimum of 1.5-fold, which may have led to the loss of valuable information and excluded genes whose more moderate changes in expression have a significant impact on translation.

5. Conclusions

In summary, the current study defines the complex gene expression profile of astrocytes in the NAWM in MS and suggests a neuroprotective role against iron-induced oxidative damage, additional functional studies would be required to fully validate this finding. Dysregulation of CNS iron levels has been linked to several neurodegenerative diseases, including Alzheimer's disease and Parkinson's disease, where current iron chelating therapeutics have been designed to block the redox-activity of iron and prevent its contribution to disease progression (Farina et al., 2013). Treatments to counteract the neurotoxic effects of iron and oxidative stress, and/or to promote astrocytic expression of MT may also potentially benefit MS patients.

Acknowledgements

Tissue samples and associated clinical and neuropathological data were supplied by the UK Multiple Sclerosis Tissue Bank, funded by the Multiple Sclerosis Society of Great Britain and Northern Ireland, registered charity 207495. We are grateful to the donors, their families, and their carers for agreement to participate in the brain donation programme. This work was supported by an educational grant from Biogen Idec.

Table 1. Age, gender, PMI, and cause of death of cases.

Case	Age (y)	Gender	PMI (h)	Cause of death
MS1*	72	F	8	Bronchopneumonia
MS2*	77	F	9	Bronchopneumonia
MS3*	86	F	11	Bronchopneumonia
MS4*	78	F	5	Metastatic carcinoma of bronchus
MS5*	46	M	7	Pneumonia
MS6	75	M	8	Cerebrovascular accident
MS7	42	F	11	Bronchopneumonia
MS8	46	M	7	Pneumonia
MS9	77	F	7	Pneumonia
MS10	73	M	8	Pneumonia
C1*	59	F	5	Bronchopneumonia
C2*	64	M	18	Cardiac failure
C3*	35	M	22	Carcinoma of the tongue
C4*	60	M	13	Ovarian cancer
C5*	69	F	33	Lung cancer
C6	35	M	22	Carcinoma of the tongue
C7	75	M	17	CVA
C8	91	F	22	Bronchial pneumonia
C9	78	F	23	Unknown

All MS cases were classified as SPMS

M, male; F, female; PMI, post mortem interval; *cases used in microarray study

Table 2. Antibody source and specificity.

Primary antibody	Isotype	Dilution	Supplier
GFAP	Rabbit IgG	1:1000	Dako, UK
S100B	Rabbit IgG	1:4000	Dako, UK
EAAT1	Mouse IgG_{2A}	1:20	Leica Microsystems, UK
EAAT2	Mouse IgG_{2A}	1:20	Leica Microsystems, UK
GS	Mouse IgG_{2A}	1:1000	Dako, UK
ALDHL1	Rabbit IgG	1:50	Abcam, UK
FTL	Rabbit IgG	1:400	Abcam, UK
CALM1	Rabbit IgG	1:100	Sigma, UK
MT	Mouse IgG	1:200	Dako, UK

IgG: immunoglobulin; GFAP: glial fibrillary acidic protein; EAAT: excitatory amino acid transporter; GS: glutamate synthetase; ALDHL1: aldehyde dehydrogenase L1; FTL: ferritin light chain; CALM1: Calmodulin; MT: metallothionein clone E9

Table 3. Genes selected to validate microarray data.

Gene		Sequence
ACTB	Probe	56-FAM/CTGCCTCCA/ZEN/CCCACTCCCA/3IABkFQ
	Primer 1	GTCCCCCAACTTGAGATGTATG
	Primer 2	AAGTCAGTGTACAGGTAAGCC
CALM1	Probe	56-FAM/CTGCTTCTC/ZEN/TGATCATTTCATTTCATCTACTTCTTCATCTG/3IABkFQ
	Primer 1	GTGCAGCAGAACTACGTCA
	Primer 2	TCTTCATTTTGCAGTCATCATCTG
FTL	Probe	56-FAM/CCTCCAGCC/ZEN/AATAGGCAGCTTTCT/3IABkFQ
	Primer 1	CTCACTCTCAAGCACGACTAAG
	Primer 2	GGTCCAAGGCTTGTTAGGATAG
MT2A	Probe	56-FAM/AGCTCGCCA/ZEN/TGGATCCCAACT/3IABkFQ
	Primer 1	AGCTTTTCTTGCAGGAGGTG
	Primer 2	GCAACCTGTCCCGACTCTA

Table 4. DAVID analysis of microarray data. Functional grouping of significant, differentially expressed genes in MS NAWM astrocytes versus control WM astrocytes.

Functional Group	Number of genes	p-value
RNA processing	19	0.013
Immunity and defence	34	0.021
Intracellular signalling cascade	28	0.0035
Protein metabolism and modification	70	0.0015
Cytoskeleton	35	0.026
Homeostasis		
Neuronal development	12	0.046
Response to metal ions	7	0.031
Cellular cation homeostasis	10	0.046
Response to hypoxia	8	0.012

Table 5. Top 20 differentially up-regulated genes. Six genes from the top 20 up-regulated genes were related to the homeostasis of iron and oxidative stress (highlighted in bold).

Probe set id	p-value	Fold change	Gene symbol	Gene Title
209619_at	0.008	2.73	CD74	CD74 molecule, major histocompatibility complex, class II invariant chain
225368_at	0.034	2.63	HIPK2	Homeodomain interacting protein kinase 2
209343_at	0.029	2.57	EFHD1	EF-hand domain family, member D1
212185_x_at	**0.032**	**2.52**	**MT2A**	**Metallothionein 2A**
225097_at	0.028	2.43	HIPK2	Homeodomain interacting protein kinase 2
204037_at	0.018	2.39	LPAR1	Lysophosphatidic acid receptor 1
225207_at	0.039	2.35	PDK4	Pyruvate dehydrogenase kinase, isozyme 4
235617_x_at	0.044	2.29	-	-
219236_at	0.027	2.28	PAQR6	Progestin and adipoQ receptor family member VI
204745_x_at	**0.031**	**2.26**	**MT1G**	**Metallothionein 1G**
205117_at	0.010	2.25	FGF1	Fibroblast growth factor 1 (acidic)
211959_at	0.024	2.24	IGFBP5	Insulin-like growth factor binding protein 5
212788_x_at	**0.030**	**2.24**	**FTL**	**Ferritin, light polypeptide**
208581_x_at	**0.042**	**2.23**	**MT1X**	**Metallothionein 1X**
229048_at	0.028	2.22	-	-
211456_x_at	**0.044**	**2.22**	**MT1P2**	**Metallothionein 1 pseudogene 2**
214064_at	**0.048**	**2.21**	**TF**	**Transferrin**
201721_s_at	0.017	2.18	LAPTM5	Lysosomal multispanning membrane protein 5
209000_s_at	0.037	2.18	SEPT8	Septin 8
218251_at	0.011	2.16	MID1IP1	MID1 interacting protein-1

Figure 1

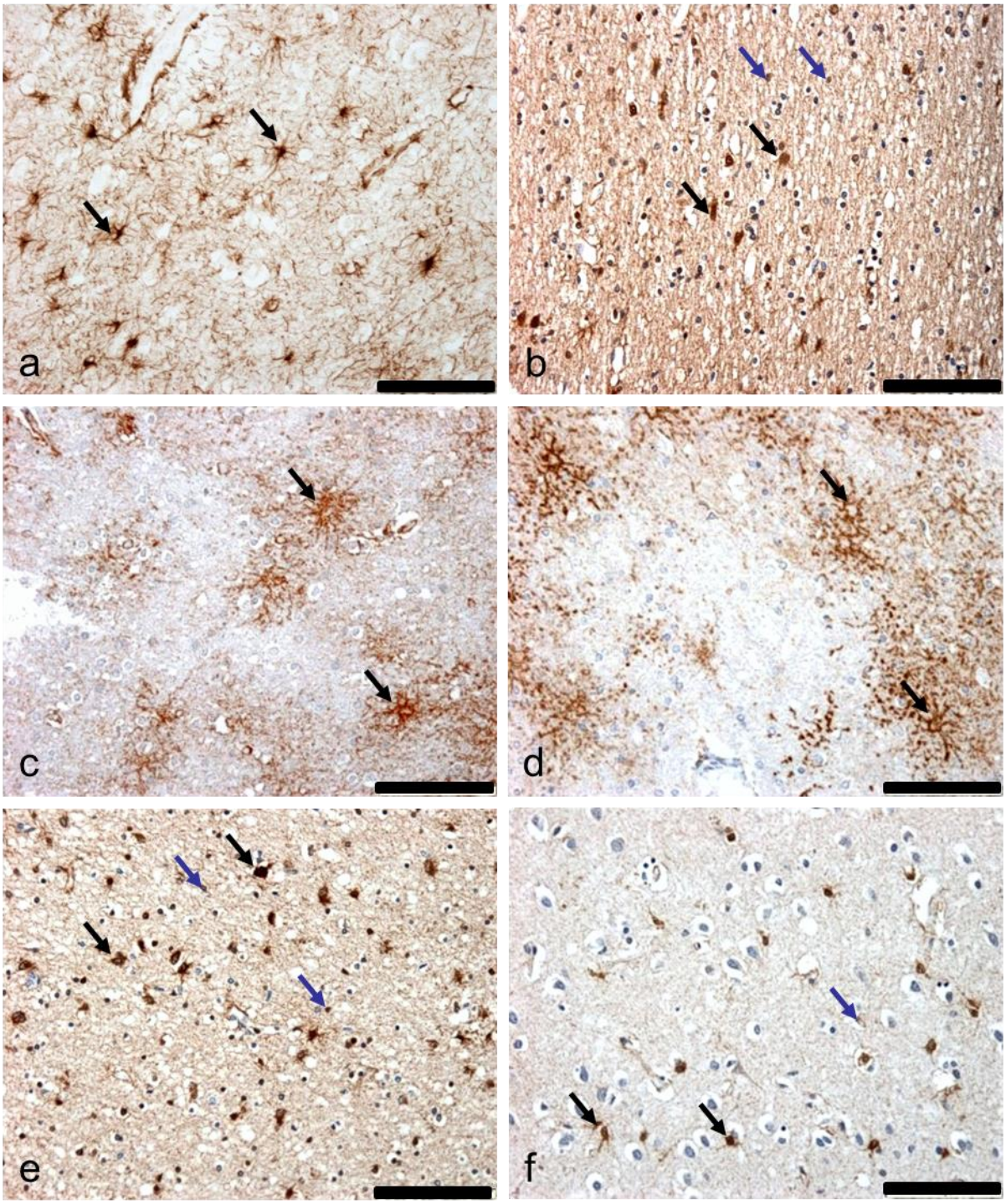

Figure 1. Immunolabelling of astrocytes. (a) GFAP$^+$ stellate astrocytes were present throughout the white matter, as indicated by the arrow. (b) S100B stained two distinct populations of cells: astrocytes (black arrow) and oligodendrocytes (blue arrow). Both (c) EAAT1 and (d) EAAT2 predominantly labelled astrocyte processes, as indicated by the arrows. (e) GS stained both astrocyte cell bodies and immediate stumpy processes (black arrow) and cells morphologically resembling oligodendrocytes (blue arrows). (f) ALDH1L1 immunoreactivity was restricted to the cortex, where it labelled both astrocytes (black arrows) and oligodendrocytes (blue arrow). Scale bar represents 100μm.

Figure 2

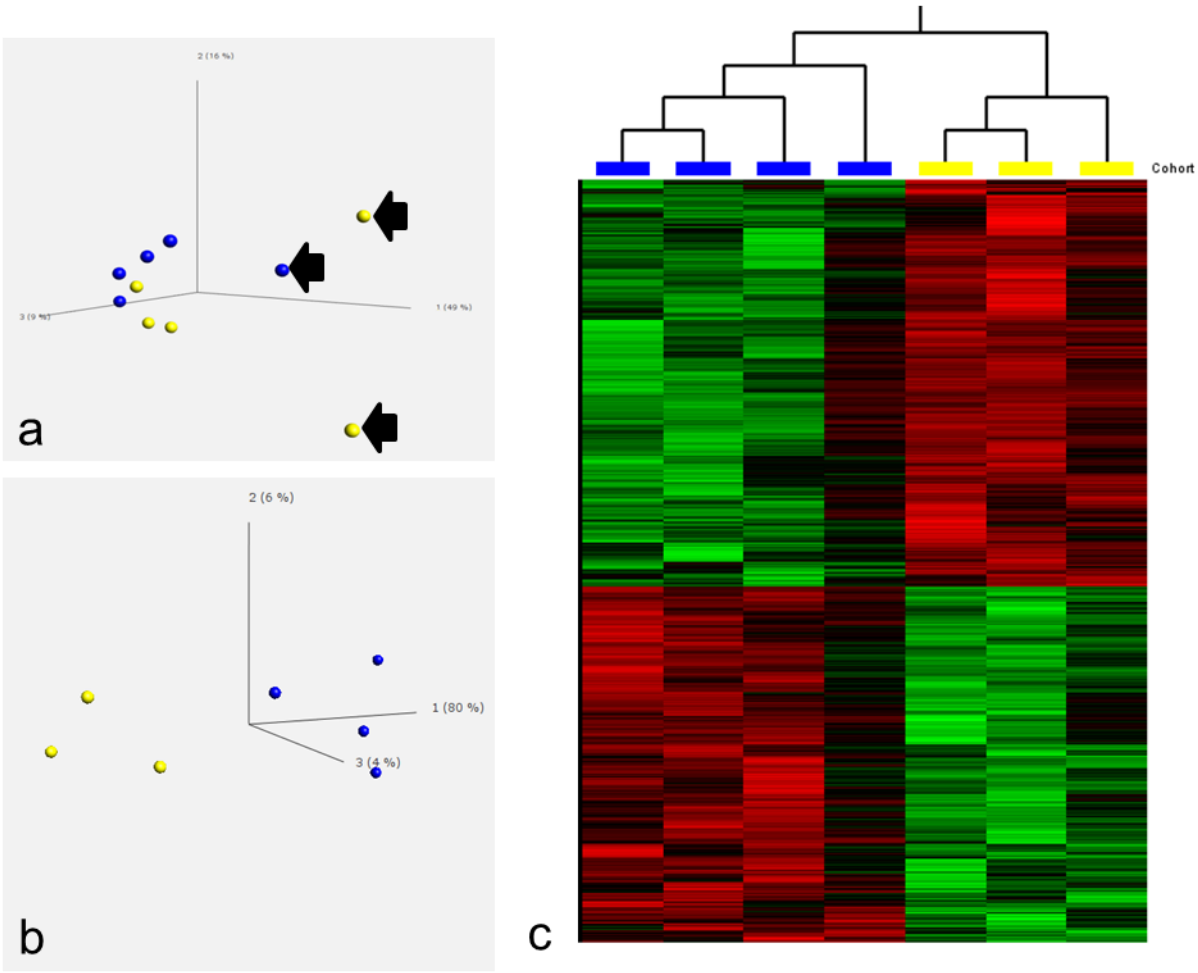

Figure 2. Gene expression analysis of the NAWM. Principal component analysis of microarray data, (a) before and (b) after three sample outliers (2 control [yellow] and 1 NAWM case [blue], indicated by the arrows) were removed from subsequent analysis. (c) Heat map depicting up-regulated (green) and down-regulated (red) gene expression changes (FC≥1.5, p≤0.05). The astrocyte transcriptome in NAWM was associated with the up-regulation of 208 genes and the down-regulation of 244 genes.

Figure 3

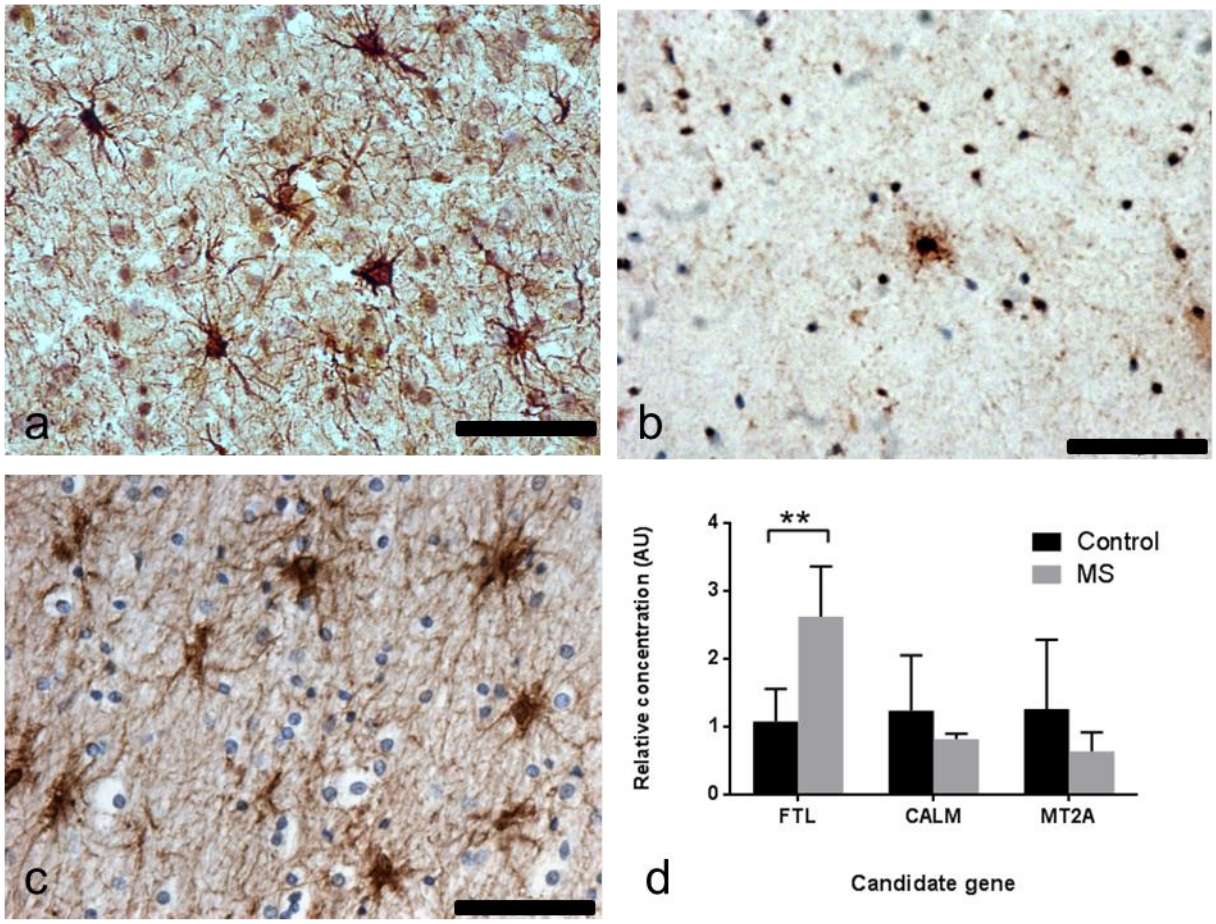

Figure 3. Confirmation of NAWM astrocytic expression of proteins encoded by candidate genes identified by the microarray analysis. (a) A proportion of FTL$^+$ cells (brown) were GFAP$^+$ (red). Both (b) CALM and (c) MT immunolabelled cells morphologically resembling astrocytes. (d) qPCR confirmed significant upregulation of *FTL* (p=0.008) and a non-significant down-regulation of *CALM* in the NAWM. Scale bar represents 50μm.

References

ALLEN, I. V. & MCKEOWN, S. R. 1979. A histological, histochemical and biochemical study of the macroscopically normal white matter in multiple sclerosis. *J Neurol Sci,* 41**,** 81-91.

ALLEN, I. V., MCQUAID, S., MIRAKHUR, M. & NEVIN, G. 2001. Pathological abnormalities in the normal-appearing white matter in multiple sclerosis. *Neurol Sci,* 22**,** 141-4.

ARGAW, A. T., ASP, L., ZHANG, J., NAVRAZHINA, K., PHAM, T., MARIANI, J. N., MAHASE, S., DUTTA, D. J., SETO, J., KRAMER, E. G., FERRARA, N., SOFRONIEW, M. V. & JOHN, G. R. 2012. Astrocyte-derived VEGF-A drives blood-brain barrier disruption in CNS inflammatory disease. *J Clin Invest,* 122**,** 2454-68.

ARGAW, A. T., ZHANG, Y., SNYDER, B. J., ZHAO, M. L., KOPP, N., LEE, S. C., RAINE, C. S., BROSNAN, C. F. & JOHN, G. R. 2006. IL-1beta regulates blood-brain barrier permeability via reactivation of the hypoxia-angiogenesis program. *J Immunol,* 177**,** 5574-84.

BAGNATO, F., HAMETNER, S., YAO, B., VAN GELDEREN, P., MERKLE, H., CANTOR, F. K., LASSMANN, H. & DUYN, J. H. 2011. Tracking iron in multiple sclerosis: a combined imaging and histopathological study at 7 Tesla. *Brain,* 134**,** 3602-15.

BAHN, S., AUGOOD, S. J., RYAN, M., STANDAERT, D. G., STARKEY, M. & EMSON, P. C. 2001. Gene expression profiling in the post-mortem human brain--no cause for dismay. *J Chem Neuroanat,* 22**,** 79-94.

BAKER, D. J., BLACKBURN, D. J., KEATINGE, M., SOKHI, D., VISKAITIS, P., HEATH, P. R., FERRAIUOLO, L., KIRBY, J. & SHAW, P. J. 2015. Lysosomal and phagocytic activity is increased in astrocytes during disease progression in the SOD1 (G93A) mouse model of amyotrophic lateral sclerosis. *Front Cell Neurosci,* 9**,** 410.

BOONE, D. R., SELL, S. L. & HELLMICH, H. L. 2013. Laser capture microdissection of enriched populations of neurons or single neurons for gene expression analysis after traumatic brain injury. *J Vis Exp*.

BRADL, M. & LASSMANN, H. 2012. Microarray analysis on archival multiple sclerosis tissue: pathogenic authenticity outweighs technical obstacles. *Neuropathology,* 32**,** 463-6.

BROSNAN, C. F. & RAINE, C. S. 2013. The astrocyte in multiple sclerosis revisited. *Glia,* 61**,** 453-65.

BSIBSI, M., PERSOON-DEEN, C., VERWER, R. W., MEEUWSEN, S., RAVID, R. & VAN NOORT, J. M. 2006. Toll-like receptor 3 on adult human astrocytes triggers production of neuroprotective mediators. *Glia,* 53**,** 688-95.

CHU, T. T., LIU, Y. & KEMETHER, E. 2009. Thalamic transcriptome screening in three psychiatric states. *J Hum Genet,* 54**,** 665-75.

CONNOR, J. R. & MENZIES, S. L. 1995. Cellular management of iron in the brain. *J Neurol Sci,* 134 Suppl**,** 33-44.

CRICHTON, R. R., DEXTER, D. T. & WARD, R. J. 2011. Brain iron metabolism and its perturbation in neurological diseases. *J Neural Transm (Vienna),* 118**,** 301-14.

CUNNEA, P., MCMAHON, J., O'CONNELL, E., MASHAYEKHI, K., FITZGERALD, U. & MCQUAID, S. 2010. Gene expression analysis of the microvascular compartment in multiple sclerosis using laser microdissected blood vessels. *Acta Neuropathol,* 119**,** 601-15.

DUTTA, R. 2013. Gene expression changes underlying cortical pathology: clues to understanding neurological disability in multiple sclerosis. *Mult Scler,* 19**,** 1249-54.

DUTTA, R., MCDONOUGH, J., CHANG, A., SWAMY, L., SIU, A., KIDD, G. J., RUDICK, R., MIRNICS, K. & TRAPP, B. D. 2007. Activation of the ciliary neurotrophic factor (CNTF) signalling pathway in cortical neurons of multiple sclerosis patients. *Brain,* 130**,** 2566-76.

DUTTA, R. & TRAPP, B. D. 2012. Gene expression profiling in multiple sclerosis brain. *Neurobiol Dis,* 45**,** 108-14.

ESPEJO, C., PENKOWA, M., DEMESTRE, M., MONTALBAN, X. & MARTINEZ-CACERES, E. M. 2005. Time-course expression of CNS inflammatory, neurodegenerative tissue repair markers and metallothioneins during experimental autoimmune encephalomyelitis. *Neuroscience,* 132**,** 1135-49.

FARINA, M., AVILA, D. S., DA ROCHA, J. B. & ASCHNER, M. 2013. Metals, oxidative stress and neurodegeneration: a focus on iron, manganese and mercury. *Neurochem Int,* 62**,** 575-94.

FLUTEAU, A., INCE, P. G., MINETT, T., MATTHEWS, F. E., BRAYNE, C., GARWOOD, C. J., RATCLIFFE, L. E., MORGAN, S., HEATH, P. R., SHAW, P. J., WHARTON, S. B., SIMPSON, J. E. & GROUP, M. R. C. C. F. A. N. S. 2015. The nuclear retention of transcription factor FOXO3a correlates with a DNA damage response and increased glutamine synthetase expression by astrocytes suggesting a neuroprotective role in the ageing brain. *Neurosci Lett,* 609**,** 11-7.

GAASCH, J. A., LOCKMAN, P. R., GELDENHUYS, W. J., ALLEN, D. D. & VAN DER SCHYF, C. J. 2007. Brain iron toxicity: differential responses of astrocytes, neurons, and endothelial cells. *Neurochem Res,* 32**,** 1196-208.

GRAUMANN, U., REYNOLDS, R., STECK, A. J. & SCHAEREN-WIEMERS, N. 2003. Molecular changes in normal appearing white matter in multiple sclerosis are characteristic of neuroprotective mechanisms against hypoxic insult. *Brain Pathol,* 13**,** 554-73.

GUERAU-DE-ARELLANO, M., LIU, Y., MEISEN, W. H., PITT, D., RACKE, M. K. & LOVETT-RACKE, A. E. 2015. Analysis of miRNA in Normal Appearing White Matter to Identify Altered CNS Pathways in Multiple Sclerosis. *J Autoimmune Disord,* 1.

HAIDER, L., FISCHER, M. T., FRISCHER, J. M., BAUER, J., HOFTBERGER, R., BOTOND, G., ESTERBAUER, H., BINDER, C. J., WITZTUM, J. L. & LASSMANN, H. 2011. Oxidative damage in multiple sclerosis lesions. *Brain,* 134**,** 1914-24.

HAMETNER, S., WIMMER, I., HAIDER, L., PFEIFENBRING, S., BRUCK, W. & LASSMANN, H. 2013. Iron and neurodegeneration in the multiple sclerosis brain. *Ann Neurol,* 74**,** 848-61.

HUANG DA, W., SHERMAN, B. T. & LEMPICKI, R. A. 2009a. Bioinformatics enrichment tools: paths toward the comprehensive functional analysis of large gene lists. *Nucleic Acids Res,* 37**,** 1-13.

HUANG DA, W., SHERMAN, B. T. & LEMPICKI, R. A. 2009b. Systematic and integrative analysis of large gene lists using DAVID bioinformatics resources. *Nat Protoc,* 4**,** 44-57.

KIERDORF, K., WANG, Y. & NEUMANN, H. 2010. Immune-mediated CNS damage. *Results Probl Cell Differ,* 51**,** 173-96.

KRIEGLSTEIN, K., STRELAU, J., SCHOBER, A., SULLIVAN, A. & UNSICKER, K. 2002. TGF-beta and the regulation of neuron survival and death. *J Physiol Paris,* 96**,** 25-30.

KUMAR, A., GIBBS, J. R., BEILINA, A., DILLMAN, A., KUMARAN, R., TRABZUNI, D., RYTEN, M., WALKER, R., SMITH, C., TRAYNOR, B. J., HARDY, J., SINGLETON, A. B. & COOKSON, M. R. 2013. Age-associated changes in gene expression in human brain and isolated neurons. *Neurobiol Aging,* 34**,** 1199-209.

KURNELLAS, M. P., DONAHUE, K. C. & ELKABES, S. 2007. Mechanisms of neuronal damage in multiple sclerosis and its animal models: role of calcium pumps and exchangers. *Biochem Soc Trans,* 35**,** 923-6.

KUTZELNIGG, A., LUCCHINETTI, C. F., STADELMANN, C., BRUCK, W., RAUSCHKA, H., BERGMANN, M., SCHMIDBAUER, M., PARISI, J. E. & LASSMANN, H. 2005. Cortical demyelination and diffuse white matter injury in multiple sclerosis. *Brain,* 128**,** 2705-12.

LEVENSON, C. W. & TASSABEHJI, N. M. 2004. Iron and ageing: an introduction to iron regulatory mechanisms. *Ageing Res Rev,* 3**,** 251-63.

LI, K. & REICHMANN, H. 2016. Role of iron in neurodegenerative diseases. *J Neural Transm (Vienna)*.

LINDBERG, R. L., DE GROOT, C. J., CERTA, U., RAVID, R., HOFFMANN, F., KAPPOS, L. & LEPPERT, D. 2004. Multiple sclerosis as a generalized CNS disease--comparative microarray analysis of normal appearing white matter and lesions in secondary progressive MS. *J Neuroimmunol,* 152**,** 154-67.

LIVAK, K. J. & SCHMITTGEN, T. D. 2001. Analysis of relative gene expression data using real-time quantitative PCR and the 2(-Delta Delta C(T)) Method. *Methods,* 25**,** 402-8.

LUND, H., KRAKAUER, M., SKIMMINGE, A., SELLEBJERG, F., GARDE, E., SIEBNER, H. R., PAULSON, O. B., HESSE, D. & HANSON, L. G. 2013. Blood-brain barrier permeability of normal appearing white matter in relapsing-remitting multiple sclerosis. *PLoS One,* 8**,** e56375.

MARZ, P., HEESE, K., DIMITRIADES-SCHMUTZ, B., ROSE-JOHN, S. & OTTEN, U. 1999. Role of interleukin-6 and soluble IL-6 receptor in region-specific induction of astrocytic differentiation and neurotrophin expression. *Glia,* 26**,** 191-200.

MASON, J. L., SUZUKI, K., CHAPLIN, D. D. & MATSUSHIMA, G. K. 2001. Interleukin-1beta promotes repair of the CNS. *J Neurosci,* 21**,** 7046-52.

MESSERSMITH, D. J., MURTIE, J. C., LE, T. Q., FROST, E. E. & ARMSTRONG, R. C. 2000. Fibroblast growth factor 2 (FGF2) and FGF receptor expression in an experimental demyelinating disease with extensive remyelination. *J Neurosci Res,* 62**,** 241-56.

MILJKOVIC, D., TIMOTIJEVIC, G. & MOSTARICA STOJKOVIC, M. 2011. Astrocytes in the tempest of multiple sclerosis. *FEBS Lett,* 585**,** 3781-8.

MINGHETTI, L. 2004. Cyclooxygenase-2 (COX-2) in inflammatory and degenerative brain diseases. *J Neuropathol Exp Neurol,* 63**,** 901-10.

MISTRY, N., TALLANTYRE, E. C., DIXON, J. E., GALAZIS, N., JASPAN, T., MORGAN, P. S., MORRIS, P. & EVANGELOU, N. 2011. Focal multiple sclerosis lesions abound in 'normal appearing white matter'. *Mult Scler,* 17**,** 1313-23.

MOLL, N. M., RIETSCH, A. M., THOMAS, S., RANSOHOFF, A. J., LEE, J. C., FOX, R., CHANG, A., RANSOHOFF, R. M. & FISHER, E. 2011. Multiple sclerosis normal-appearing white matter: pathology-imaging correlations. *Ann Neurol,* 70**,** 764-73.

MOORE, C. S., ABDULLAH, S. L., BROWN, A., ARULPRAGASAM, A. & CROCKER, S. J. 2011a. How factors secreted from astrocytes impact myelin repair. *J Neurosci Res,* 89**,** 13-21.

MOORE, C. S., MILNER, R., NISHIYAMA, A., FRAUSTO, R. F., SERWANSKI, D. R., PAGARIGAN, R. R., WHITTON, J. L., MILLER, R. H. & CROCKER, S. J. 2011b. Astrocytic tissue inhibitor of metalloproteinase-1 (TIMP-1) promotes oligodendrocyte differentiation and enhances CNS myelination. *J Neurosci,* 31**,** 6247-54.

MYCKO, M. P., BROSNAN, C. F., RAINE, C. S., FENDLER, W. & SELMAJ, K. W. 2012. Transcriptional profiling of microdissected areas of active multiple sclerosis lesions reveals activation of heat shock protein genes. *J Neurosci Res,* 90**,** 1941-8.

NAIR, A., FREDERICK, T. J. & MILLER, S. D. 2008. Astrocytes in multiple sclerosis: a product of their environment. *Cell Mol Life Sci,* 65**,** 2702-20.

PEKNY, M., PEKNA, M., MESSING, A., STEINHAUSER, C., LEE, J. M., PARPURA, V., HOL, E. M., SOFRONIEW, M. V. & VERKHRATSKY, A. 2015. Astrocytes: a central element in neurological diseases. *Acta Neuropathol*.

PENKOWA, M., ESPEJO, C., ORTEGA-AZNAR, A., HIDALGO, J., MONTALBAN, X. & MARTINEZ CACERES, E. M. 2003. Metallothionein expression in the central nervous system of multiple sclerosis patients. *Cell Mol Life Sci,* 60**,** 1258-66.

PENKOWA, M. & HIDALGO, J. 2000. Metallothionein I+II expression and their role in experimental autoimmune encephalomyelitis. *Glia,* 32**,** 247-63.

PENKOWA, M. & HIDALGO, J. 2001. Metallothionein treatment reduces proinflammatory cytokines IL-6 and TNF-alpha and apoptotic cell death during experimental autoimmune encephalomyelitis (EAE). *Exp Neurol,* 170**,** 1-14.

PENKOWA, M. & HIDALGO, J. 2003. Treatment with metallothionein prevents demyelination and axonal damage and increases oligodendrocyte precursors and tissue repair during experimental autoimmune encephalomyelitis. *J Neurosci Res,* 72**,** 574-86.

PIETERSEN, C. Y., LIM, M. P. & WOO, T. U. 2009. Obtaining high quality RNA from single cell populations in human postmortem brain tissue. *J Vis Exp*.

SARCHIELLI, P., DI FILIPPO, M., ERCOLANI, M. V., CHIASSERINI, D., MATTIONI, A., BONUCCI, M., TENAGLIA, S., EUSEBI, P. & CALABRESI, P. 2008. Fibroblast growth factor-2 levels are elevated in the cerebrospinal fluid of multiple sclerosis patients. *Neurosci Lett,* 435**,** 223-8.

SIMPSON, J. E., INCE, P. G., MINETT, T., MATTHEWS, F. E., HEATH, P. R., SHAW, P. J., GOODALL, E., GARWOOD, C. J., RATCLIFFE, L. E., BRAYNE, C., RATTRAY, M., WHARTON, S. B., FUNCTION, M. R. C. C. & AGEING NEUROPATHOLOGY STUDY, G. 2015. Neuronal DNA damage response-

associated dysregulation of signalling pathways and cholesterol metabolism at the earliest stages of Alzheimer-type pathology. *Neuropathol Appl Neurobiol*.

SIMPSON, J. E., INCE, P. G., SHAW, P. J., HEATH, P. R., RAMAN, R., GARWOOD, C. J., GELSTHORPE, C., BAXTER, L., FORSTER, G., MATTHEWS, F. E., BRAYNE, C., WHARTON, S. B., FUNCTION, M. R. C. C. & AGEING NEUROPATHOLOGY STUDY, G. 2011. Microarray analysis of the astrocyte transcriptome in the aging brain: relationship to Alzheimer's pathology and APOE genotype. *Neurobiol Aging,* 32**,** 1795-807.

SOFRONIEW, M. V. & VINTERS, H. V. 2010. Astrocytes: biology and pathology. *Acta Neuropathol,* 119**,** 7-35.

STABLES, M. J., NEWSON, J., AYOUB, S. S., BROWN, J., HYAMS, C. J. & GILROY, D. W. 2010. Priming innate immune responses to infection by cyclooxygenase inhibition kills antibiotic-susceptible and -resistant bacteria. *Blood,* 116**,** 2950-9.

TODORICH, B., PASQUINI, J. M., GARCIA, C. I., PAEZ, P. M. & CONNOR, J. R. 2009. Oligodendrocytes and myelination: the role of iron. *Glia,* 57**,** 467-78.

WALLER, R., WOODROOFE, M. N., FRANCESE, S., HEATH, P. R., WHARTON, S. B., INCE, P. G., SHARRACK, B. & SIMPSON, J. E. 2012. Isolation of enriched glial populations from post-mortem human CNS material by immuno-laser capture microdissection. *J Neurosci Methods,* 208**,** 108-13.

WHITNEY, L. W., BECKER, K. G., TRESSER, N. J., CABALLERO-RAMOS, C. I., MUNSON, P. J., PRABHU, V. V., TRENT, J. M., MCFARLAND, H. F. & BIDDISON, W. E. 1999. Analysis of gene expression in mutiple sclerosis lesions using cDNA microarrays. *Ann Neurol,* 46**,** 425-8.

WILLIAMS, A., PIATON, G. & LUBETZKI, C. 2007. Astrocytes--friends or foes in multiple sclerosis? *Glia,* 55**,** 1300-12.

WILLIAMS, R., BUCHHEIT, C. L., BERMAN, N. E. & LEVINE, S. M. 2012. Pathogenic implications of iron accumulation in multiple sclerosis. *J Neurochem,* 120**,** 7-25.

ZEIS, T., GRAUMANN, U., REYNOLDS, R. & SCHAEREN-WIEMERS, N. 2008. Normal-appearing white matter in multiple sclerosis is in a subtle balance between inflammation and neuroprotection. *Brain,* 131**,** 288-303.